Desalination and Water Treatment
www.deswater.com

doi: 10.5004/dwt.2022.28316

255 (2022) 4–12
April

Performance optimization and reliability of solar pumping system designed for smart agriculture irrigation

Yahia Serbouh[a,*], Taha Benikhelef[a], Djamel Benazzouz[a], Mohamed Abdessamed Ait Chikh[a], Sami Touil[b], Amina Richa[b], Hacene Mahmoudi[c]

[a]*Faculty of Technology, M'hamed Bougara University, Boumerdes, Algeria, emails: y.serbouh@univ-boumerdes.dz (Y. Serbouh), taha.yacine@gmail.com (T. Benikhelef), dbenazzouz@yahoo.fr (D. Benazzouz), m.aitchikh@univ-boumerdes.dz (M.A. Ait Chikh)*
[b]*University of Djilali Bounaama, Khemis Miliana, Algeria, emails: s.touil@univ-dbkm.dz (S. Touil), a.richa@univ-dbkm.dz (A. Richa)*
[c]*Faculty of Technology, University Hassiba Benbouali of Chlef, Algeria, email: h.mahmoudi@univ-chlef.dz (H. Mahmoudi)*

Received 29 July 2021; Accepted 23 December 2021

ABSTRACT

The aim of the study was to employ mathematical modeling in the analysis of a photovoltaic (PV) water pumping system designed for smart agriculture irrigation that combines crops in the ground with PV panels (i.e., agrivoltaic), using as a case study the region of Khemis Miliana in Algeria in northwest Africa. System performance was optimized by considering the variation in solar irradiance level, ambient temperature, generated PV power, pump flow rate and head, and water demand for irrigation. The maximum power point tracking (MPPT) of the PV module was estimated from the I-V curve model. The performance equation that expresses the flow rate of the pump as a function of input power and the total head was modeled based on the manufacturer's performance curves using a feed-forward backpropagation network. Results showed that an increase in irradiance intensity increased the pump flow rate. A higher head gave a lower flow rate, regardless of the change in solar irradiance intensity. The power excess was predicted monthly. This power can be further utilized for secondary applications. The PV water pumping arrangement model enables advance estimation of system outputs and allows for optimization and improvement in the performance and reliability, accounting for variation in solar irradiance level, different pump operating parameters, and the water demand for irrigation. Future studies are suggested on excess power analysis including economics and considering the targeted plants to better optimize the system in terms of water need and frequency for irrigation.

Keywords: Agrivoltaic (APV); Intelligent irrigation; Integrity; Performance optimization; Photovoltaic (PV); Reliability; Smart agriculture; Solar pumping system

1. Introduction

A system that combines crops in the ground with photovoltaic (PV) panels installed a few meters above the ground is called an agrivoltaic system [1]. Agrivoltaic systems are a key technology for achieving sustainable development goals by reducing the use of land for food vs. land for energy. Agrivoltaic systems are at the core of the balance between electricity generation, agricultural production, and irrigation water savings [2]. Agrivoltaic systems provide a solution to the growing demand for food and energy while reducing water consumption [3]. Furthermore, an agrivoltaic farm can be used as a stand-alone energy source to water pumping systems for irrigation in areas where the electrical grid is insufficient or non-existent [4].

Smart agriculture can enhance agricultural performance in a more effective and sustainable manner [5]. Therefore, a reliable and economical irrigation system is needed.

* Corresponding author.

Presented at the International Virtual Conference on Water and Energy (ICWE 21), Hassiba Benbouali University of Chlef, Algeria, 25–27 May 2021

Irrigation level management plays a very important role in saving water for different purposes and using it economically. More than 25% of water is wasted while using traditional irrigation methods [6]. An improved irrigation system can save a large amount of water that is being wasted due to improper water management. Hence, the need for a reliable and economical irrigation system. Photovoltaic (PV) pumping systems are considered as an alternative approach to water supply for irrigation [7].

With the growing awareness of an emerging energy crisis in the world, solar-powered water pumping systems have been a focal point for researchers for decades.

Verma et al. [8] presented an extensive overview of the solar photovoltaic powered water pumping system, its major elements, and applications. Economic and environmental considerations were also addressed. Gasque et al. [9] analyzed a method of distributing the generated power in a photovoltaic pumping system having two identical pumps, working in parallel to determine a strategy for distributing the generated power that maximizes the flow rate of the two pumps together. Salilih et al. [10] proposed a method for the modelling, simulation and analysis of solar PV water pumping system. Bhayo et al. [11] presented a mathematically based evaluation procedure for a reliable, stand-alone PV-battery water pumping system to evaluate the function of the proposed system for a rural housing unit in Malaysia. Renu et al. [12] suggested a methodology for optimizing the performance of solar photovoltaic pumps by considering the effect of irradiance and temperature variations and different grid configurations on the performance of the water pump. Santra [13] evaluated experimentally a solar PV pumping system used for irrigation purpose in India. Statkic et al. [14] performed a selection procedure to identify the most significant factors for predicting the performance of the photovoltaic pumping system, by analyzing which factors have the most effect on the performance ratio to perform a satisfactory calibration to decrease the system losses. Adaptive neuro fuzzy inference system has been used for this purpose.

Sontake et al. [15] conducted a comparative study to investigate the head effect on the optimum photovoltaic array configuration, pump and pumping system total efficiency by performing experiment on the centrifugal deep well pump, with different photovoltaic modules configuration. Sontake et al. [16] performed an experimental investigation to select the optimum photovoltaic array configuration (PVAC) to supply electric power to solar photovoltaic water pumping system (SPVWPS) and effect of seasonal variations on its output by investigating the performance of SPVWPS with different PVACs. Benghanem et al. [17] developed experimentally a model that highlight the relation between water flow rate and solar power for system performance prediction. The PV pumping system efficiency is highly impacted by the climatic conditions which vary throughout the day and the year [18]. Hence, the need for a reliable and validated model taking into consideration all the variables and constraints.

The aim of the current study was to employ mathematical modeling in the analysis of a photovoltaic (PV) water pumping system designed for smart agriculture irrigation, using as a case study the region of Khemis Miliana in Algeria in northwest Africa. System performance was optimized by considering the variation in solar irradiance level, ambient temperature, generated PV power, pump flow rate and head, and water demand for irrigation. The maximum power point tracking (MPPT) of the PV module was estimated from the I-V curve model using the single diode model of the PV cell, then, the pump performance characteristic was modeled based on the manufacturer performance curve using feed-forward backpropagation network. The hourly irradiance data (G) and the ambient temperature were collected for each day for 12 months, and the average value was calculated along with the PV cell temperature. The model was then simulated to obtain the hourly produced power, the average monthly flow rates, and the guaranteed volume. Finally, the quantity of PV module which satisfies the daily required volume was defined and the average monthly power excess was calculated.

2. System modeling

The principal system elements of the solar photovoltaic water pumping system considered are the photovoltaic modules, the centrifugal pump, and a water storage tank with a capacity of 23 m^3 used instead of storage batteries. In this section, the modeling of the system is presented.

2.1. Photovoltaic module modeling

To be able to evaluate the performance of a PV system, we first need to understand the detailed electrical characteristics of the PV module. Hence, modeling is essential. The modeling of PV module involves a range of parameters provided by the manufacturer's data sheet (Table 1). For example, the maximum power current (I_{mp}) required is 9.68 A.

The equation that describes the I-V characteristic mathematically is defined based on the single diode model of the PV cell (Fig. 1) [19].

$$I = I_{pv} - I_0\left[\exp\left(\frac{V + IR_s}{aN_sV_t}\right) - 1\right] - \frac{V + IR_S}{R_p} \tag{1}$$

The light-generated current I_{pv} is expressed in function of the nominal light current $I_{pv,n}$, both are calculated using Eqs. (2) and (3) respectively [20].

$$I_{pv} = \left(I_{Pv,n} + K_{Isc}\left(T - T_n\right)\right)\frac{G}{G_{amb}} \tag{2}$$

$$I_{Pv,n} = \frac{R_p + R_S}{R_p} I_{Sc,n} \tag{3}$$

The PV cell temperature varies with the ambient temperature and solar irradiance as presented in Eq. (4) [21].

$$T = T_a + \frac{G_{amb}\left(T_{NOCT} - T_{a,NOCT}\right)}{G_{NOCT}} \tag{4}$$

The diode saturation current and the nominal saturation current can be expressed by the following [22]:

Table 1
PV module specification

Module type	JKM325M-60-V
Cell type	Mono PERC 158.75 mm × 158.75 mm
No. of cells	60 (6 × 10)
Dimensions	1,665 mm × 1,002 mm × 30 mm
Maximum power (P_{max})	325 Wp
Maximum power voltage (V_{mp})	33.6 V
Maximum power current (I_{mp})	9.68 A
Open-circuit voltage (V_{oc})	41.1 V
Short-circuit current (I_{sc})	10.50 A
Operating temperature (°C)	–40°C~+85°C
Temperature coefficients of P_{max}	–0.37%/°C
Temperature coefficients of V_{oc}	–0.29%/°C
Temperature coefficients of I_{sc}	0.048%/°C
Nominal operating cell temperature (NOCT)	45°C ± 2°C

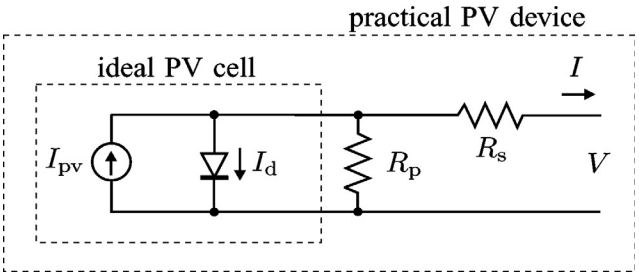

Fig. 1. Single-diode model of the theoretical PV cell and equivalent circuit of a practical PV device.

$$I_0 = I_{0,n}\left(\frac{T_n}{T}\right)^3 \exp\left[\frac{qE_g}{ak}\left(\frac{1}{T_n}-\frac{1}{T}\right)\right] \tag{5}$$

$$I_{0,n} = \frac{I_{sc,n}}{\exp\left(\frac{V_{oc}}{aV_{t,n}}\right)-1} \tag{6}$$

The thermal voltage and nominal thermal of the module are calculated as below [23]:

$$V_{t,n} = K\frac{T_n}{q} \tag{7}$$

$$V_t = K\frac{T}{q} \tag{8}$$

2.2. Experimental project description and weather data modeling

The agrivoltaic system studied in this paper is part of the WATERMAD 4.0 project. It provides an overview of the agrivoltaic technology, and the system design steps. The Algerian pilot project at the University of Khemis Miliana research site would offer the possibility to analyze the potential of agrivoltaic application to provide energy to isolated areas and to reduce irrigation needs through shading and test opportunities to integrate smart irrigation systems into the mounting structure of the agrivoltaic system. The modules are mono-facial polycrystalline and are produced by Chinese manufacturer Jinko Solar. The pump considered in this study is manufactured by Grundfos. This study was conducted under the meteorological conditions of the city of Khemis Miliana in Algeria, which is located on coordinates of 36° of latitude and 2° of longitude. The climatic data such as irradiance and ambient temperature were collected hourly for 365 d during the year of 2019, accordingly, the monthly average of irradiance and ambient temperature was calculated. The cell temperature was also calculated based on Eq. (4).

2.3. Pump performance modeling

The Pump performance is modeled based on the performance equation that expresses the flow rate of the pump as a function of input power and the total head which is represented by the pump performance curves (Fig. 2). Where *X*-axis represents the pump electric power, and *Y*-axis (left side) the pump flowrate while *Y*-axis (right side) the pump efficiency, and for different value of pump head (from 30 to 70 m).

The pump characteristic model was extracted from the performance curves provided by the pump manufacturer. The features are the electrical power and head, whereas the flow rate is considered as target, all the training and testing data points were extracted from the performance curves of the pumps (Fig. 2). The model was created by a feed-forward backpropagation network [24,25] using MATLAB toolbox. With three hidden layers and seven neurons of each one, the absolute error between the model output and target is about 0.63%.

Fig. 3 represents the back-propagation neural network architecture.

The first step was computing the output of each layer from input x into the output y according to the flowing equation:

$$a^{m+1} = F^{m+1}\left(W^{m+1}a^m + b^{m+1}\right) \tag{9}$$

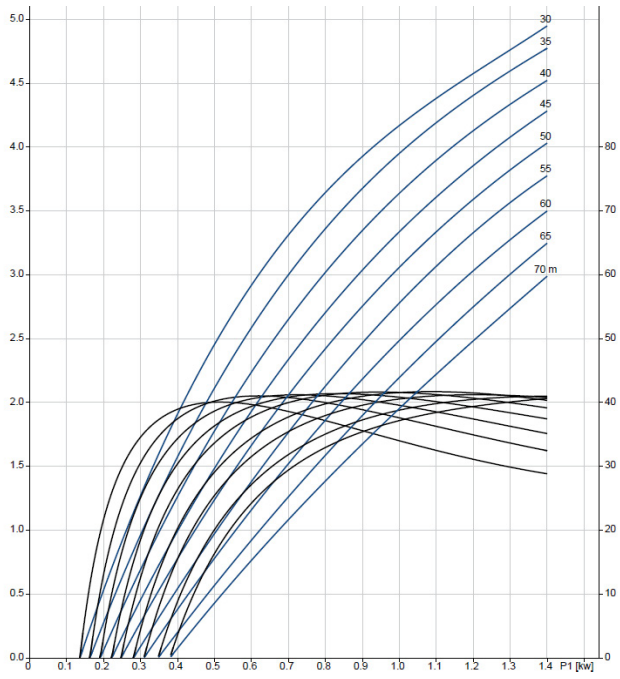

Fig. 2. Performance curves of the pump (SQF 3A-10NRp – Grundfos).

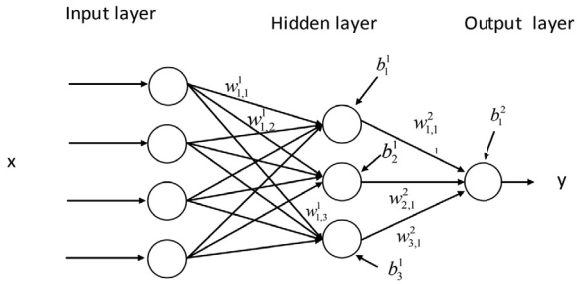

Fig. 3. Back-propagation neural network architecture.

where $m = 0, 1, \ldots M–1$.

$$n_i^m = \sum_{j=1}^{\mathrm{NR}^{m-1}} w_{i,j}^m a_j^{m-1} + b_i^m \tag{10}$$

NR: Number of neurons; M: Number of layers; B: Bias vector of different layers; W: Weight matrix of different layers.

At $m = 0$; $a = x$.

At $m+1 = M$; $a = y$.

F is the activation function at $m+1$ layer.

The second step was the back propagation for adjusting the weight w, that is, based on the sensitivities backward "S" through the network:

$$\begin{aligned} s^M &= -2F^{n^M} n^M \left(y_t - y\right) \\ s^M &= -2F^{nM}\left(n^m\right)\left(w^{m+1}\right)^T S^{m+1} \end{aligned} \tag{11}$$

y_t is the target data.

$m = M–1, \ldots, 2, 1$.

$$F^{N^M}\left(n^m\right) = \begin{bmatrix} F^{N^M}\left(n_1^m\right) & 0 & \cdots & 0 \\ 0 & F^{N^M}\left(n_1^m\right) & \cdots & 0 \\ 0 & 0 & \cdots & F^{N^M}\left(n_{\mathrm{NR}^m}^m\right) \end{bmatrix} \tag{12}$$

$$F^{N^M}\left(n_j^m\right) = \frac{\partial f^m\left(n_j^m\right)}{\partial n_j^m} \tag{13}$$

Finally, the weights matrices and biases vectors were updated using the approximate steepest descent rule:

$$\begin{aligned} W^m(k+1) &= W^m(k) - \alpha s^m \left(a^{m-1}\right)^T \\ b^m(k+1) &= b^m(k) - \alpha s^m \end{aligned} \tag{14}$$

where α is the learning rate.

The obtained modeled curves are represented in Fig. 4.

3. Results and discussion

The results of the modeling equations developed in Section 2 will be described in this section. The PV module generated electrical outputs, as well as the hourly variation of the PV pumping system's performance, will be discussed.

3.1. Variation in average irradiance, ambient and cell temperatures

The monthly average of irradiance and ambient temperature which were calculated based on the meteorological data collected at site are presented by Figs. 5 and 6. For example, in January at 14 h the average irradiation was 800 W/m^2 and the ambient temperature was 11°C, respectively. The cell temperature, calculated based on Eq. (4), is represented in Fig. 7. For example, in July at 10 h the cell temperature is 40°C, while in January for cell temperature will be 5°C during the same time, that is, 10 h.

3.2. PV pumping system medelling results

Figs. 8 and 9 present modelling results for I-V and P-V characteristics of the PV module at 25°C cell temperature for varying irradiance level. The data shows that PV module exhibits a nonlinear I-V and P-V characteristics which vary with the irradiance intensity and cell temperature. Fig. 8 presents modelling results for electrical characteristics of the PV module on current vs. voltage for different irradiance value. From the figure it can be seen that the short circuit current (I_{sc}) increases significantly with the increase of irradiance level, while it has less effect on the open circuit voltage (V_{oc}) of the PV module.

The proposed model of the PV module I-V and P-V characteristic curves is compared to manufacturer's experimental data which is available in Appendix A. The I-V and P-V characteristics (i.e., solid lines) predicted by our model closely matched those from the experimental results (i.e., dashed lines) achieved by the manufacturer, as shown in Figs. 10 and 11. The number of modules required to achieve the requested volume of 23 m^3 of the storage tank number of PV module was defined based on the worst-case scenario,

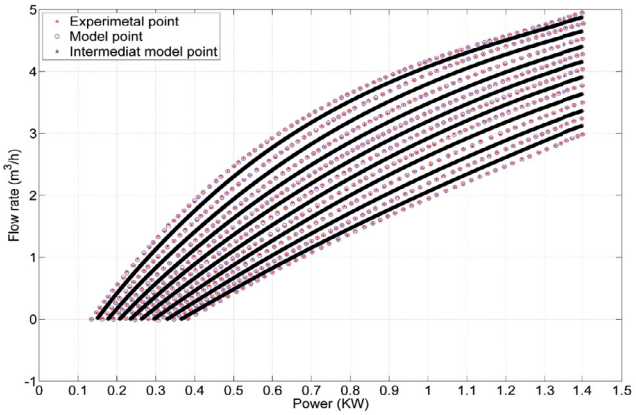

Fig. 4. Pump performance curves and extracted model.

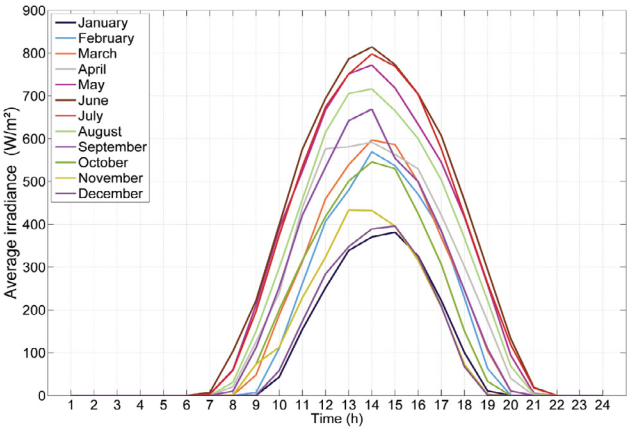

Fig. 5. Average hourly irradiance variation.

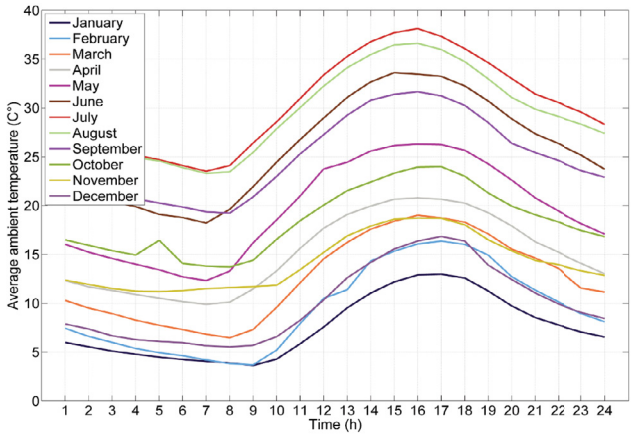

Fig. 6. Average hourly ambient temperature variation.

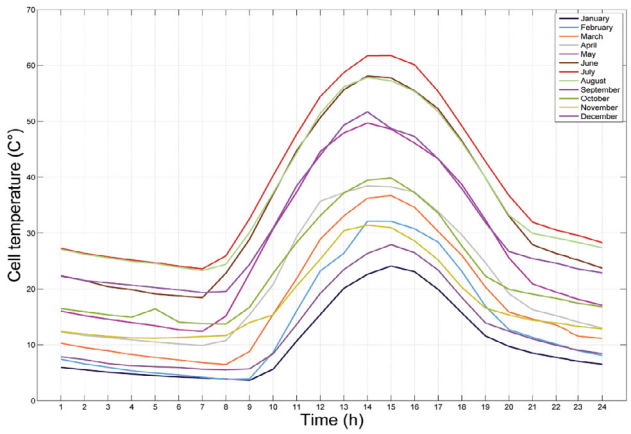

Fig. 7. Calculated hourly PV cell temperature variation.

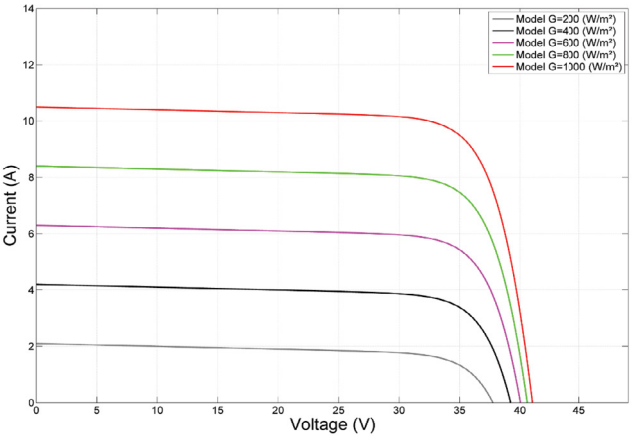

Fig. 8. I-V characteristics for different irradiance values.

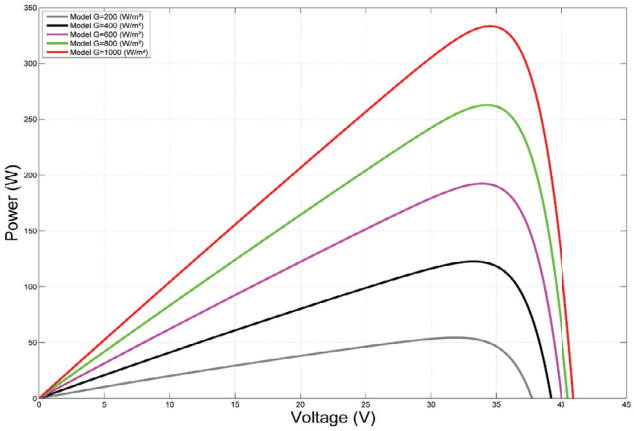

Fig. 9. P-V characteristics for different irradiance values.

that is, the month with the minimum irradiance level the same has been optimized to 10 modules.

It can be observed that Figs. 12–15 have similar trend as that of the average hourly irradiance variation in Fig. 5. The hourly predicted power of PV modules is represented by Fig. 12, where the maximum power point is selected. The results indicates that the maximum power was in the month of June while the minimum power was in the month of January. The hourly estimated flow rate for each month and for various head values is depicted in Figs. 13–15. An increase in irradiance intensity results in an increase in pump flow rate, but a higher head result in a lower flow rate regardless of the change in solar irradiance intensity.

The pump operating time is represented by Fig. 16, the minimum avergae working time is 7 h during the month of December, while the maximum operating time is 13 h

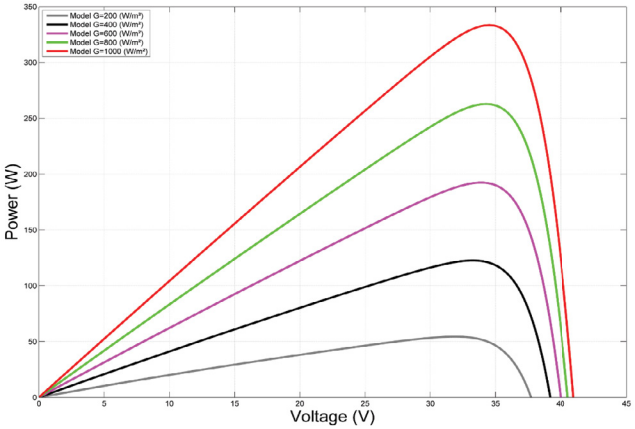

Fig. 10. I-V characteristics of proposed model and experimental data.

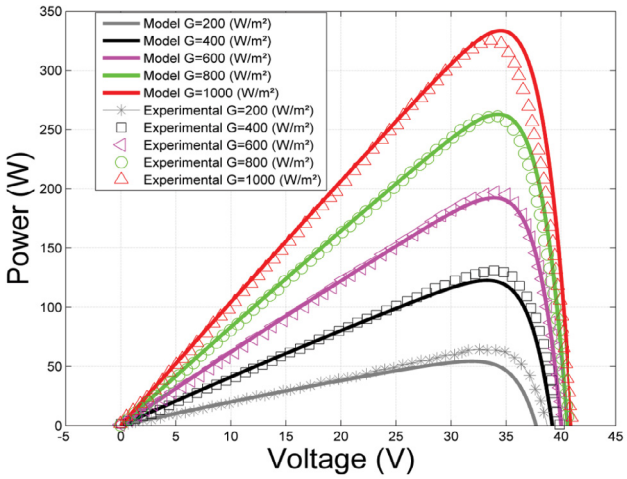

Fig. 11. P-V characteristics of proposed model and experimental data.

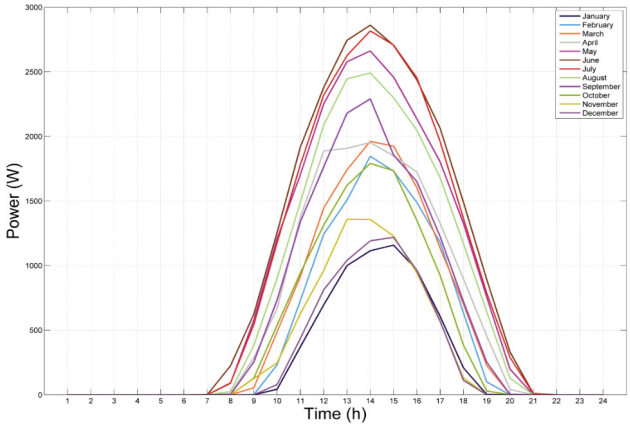

Fig. 12. Hourly predicted PV power variation.

during the month of June. Figs. 17 and 18 represent the average monthly flow rate and the average monthly guaranteed volume respectively. The average monthly flow rate (Fig. 17) vary from its minimum value in the month

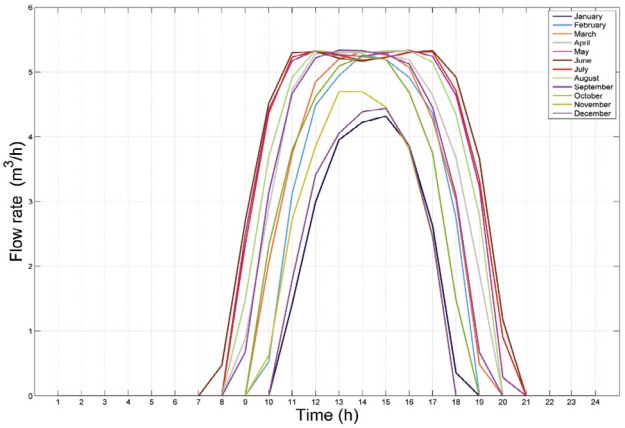

Fig. 13. Hourly predicted flow rate variation for $H = 35$ m.

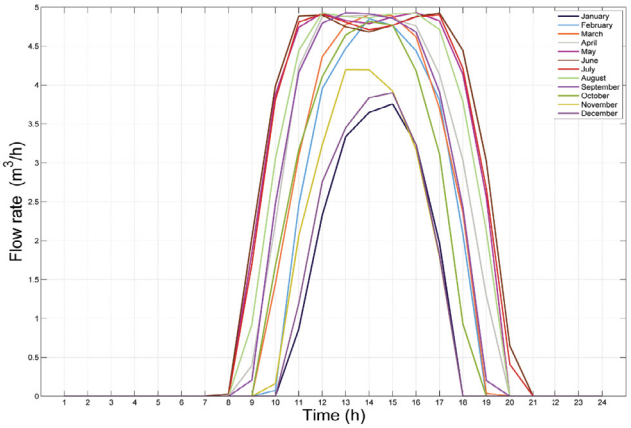

Fig. 14. Hourly predicted flow rate variation for $H = 45$ m.

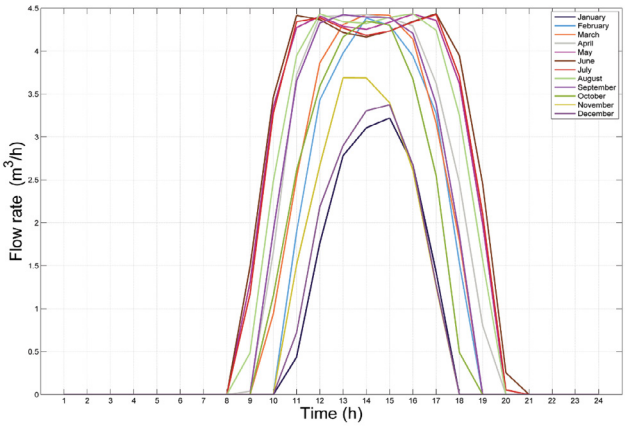

Fig. 15. Hourly predicted flow rate variation for $H = 55$ m.

of January (less than 3 m^3/h) to its maximum value in the month of August (~4.44 m^3/h). The average monthly guaranteed volume (Fig. 18) increases from les than 25 m^3 in the month of January to its maximum value (~54 m^3) in the month of June, and then decreases to less than 25 m^3 in the month of December. The system was designed for the month of January which has the minimum power (i.e., less than 800 W) as shown in Fig. 19. The model allows

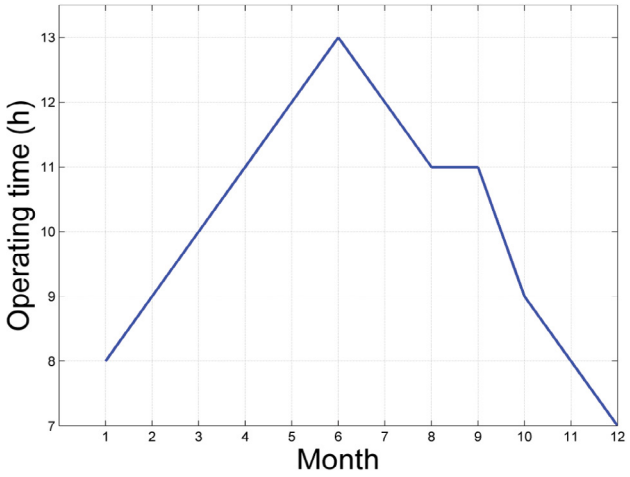

Fig. 16. Average monthly pump operating time.

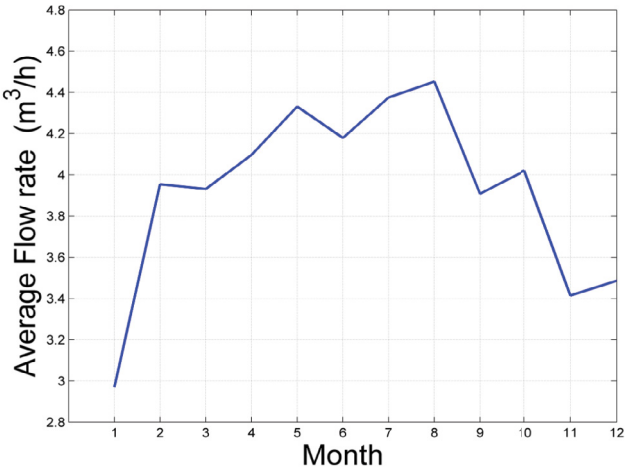

Fig. 17. Average monthly flow rate.

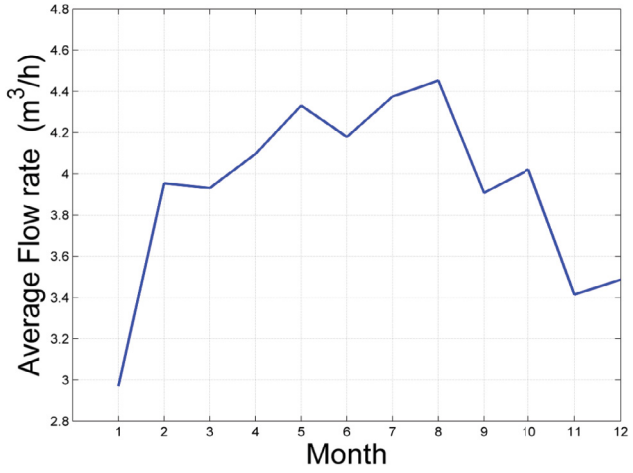

Fig. 18. Average monthly guaranteed volume.

for predicting the excess of power produced every month. The maximum excess power was around 970 W during the month of July as highlighted in Table 2 and Fig. 20.

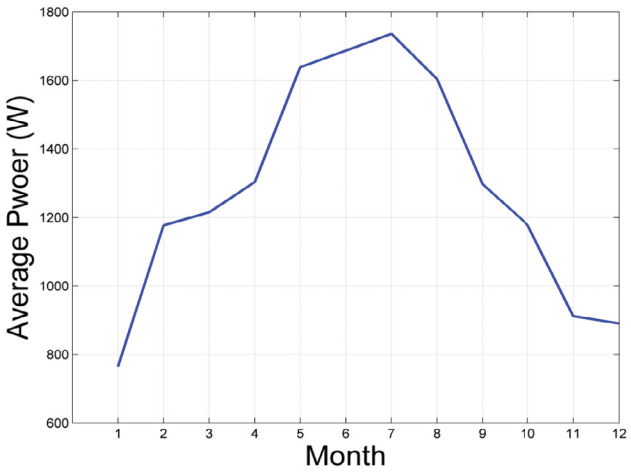

Fig. 19. Average monthly available power.

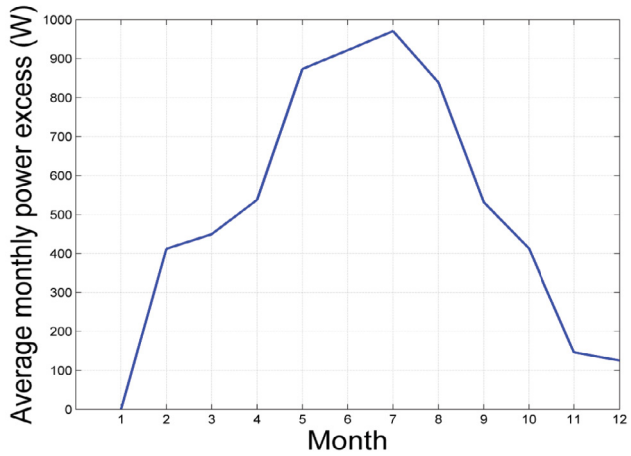

Fig. 20. Average monthly power excess.

4. System integrity and reliability

The PV water pumping arrangement model developed in the current study enables advance estimation of system outputs and allows for optimization and improvement in the performance, reliability, and integrity, accounting for variation in solar irradiance level, different pump operating parameters, and the water demand for irrigation. To achieve a high degree of integrity and reliability of the PV pumping system it is crucial to address any possible operational and safety issues. This can be accomplished through an engineering tool called reliability, availability, and maintainability (RAM). Its goal is to discover a system's weakest points to improve overall system reliability [26]. This was demonstrated by Sayed et al. [26], in an analysis for grid-connected solar photovoltaic systems. The authors concluded that the monitoring of the critical subassemblies of a PV system will increase the possibility not only for improving the availability of the system, but also to optimize the maintenance costs. Additionally, it would inform the operators about the status of the various subsystems of the system. We can speculate that the RAM approach should be implemented in the analysis of a photovoltaic (PV) water pumping system

Table 2
Monthly average excess power

Month	Average excess power (W)
Jan	0
Feb	411.82
Mar	449.60
Apr	537.7
May	873.54
June	921.79
Jul	970.86
Aug	838.76
Sep	531.97
Oct	412.76
Nov	146.39
Dec	125.38

designed for smart agriculture irrigation that combines crops in the ground with PV panels (i.e., agrivoltaic) using as a case study, for instance, the region of Khemis Miliana in Algeria in northwest Africa

In a related report Altamimi and Jayaweera [27] argued that the accelerating rate of climate change is likely to impact the performance of photovoltaic (PV) power generating systems over the long run. Their paper proposed a long-term reliability assessment approach for PV integrated power systems by considering the climate change effects on hierarchical level of PV systems. They concluded that the ability of identifying the critical components and subsystems in a PV system that lead to climate associated failures is one of the key benefits of the approach. In their investigation, two established climate models were incorporated to generate climate change factors for the years 2020, 2050 and 2080. A set of case studies were conducted, and the results suggested that the reliability performance decreases considerably with the effects of climate change. These effects were inconsistent over time when aging was taken into consideration. Their conclusions should be considered when designing future reliability proposals involving agrivoltaic systems as reported in the present report.

Capacity building can contribute for better management of the solar driven pumping system. Mahmoudi et al. [28] highlighted the importance of the capacity building in the renewable energy application such as water desalination.

5. Conclusions

The mathematical modeling analysis of a photovoltaic water pumping system designed for smart agriculture irrigation in the region of Khemis Miliana, Algeria in northwest Africa, showed that an increase in irradiance intensity increased the pump flow rate. A higher head gave a lower flow rate, regardless of the change in solar irradiance intensity. The number of PV modules was defined and optimized to satisfy the required water demand. The power excess was predicted monthly, this power can be further utilized for secondary applications. The PV water pumping system model enables advance estimation of system outputs and allows for optimization and improvement in the performance and the integrity of the system, accounting for variation in solar irradiance level, different pump operating parameters, and the water demand for irrigation. Future studies are suggested on excess power economic analysis and on considering the targeted plants to better optimize the system in terms of water need and frequency for irrigation.

Acknowledgments

This study was funded by PRIMA programme supported by the European Union under Grant Agreement number: [1821] [WATERMED] [Call 2018 Section 1 Water]. We appreciate the support provided by General Directorate for Scientific Research and Technological Development (DGRSDT).

Declarations

Conflict of interest: The authors declare that they have no conflict of interest.

Symbols

a	—	Ideality factor
E_g	—	Bandgap energy of the semiconductor, eV
G_{amb}	—	Solar irradiance at ambient temperature, W/m^2
G_{NOCT}	—	Solar irradiance, W/m^2
I	—	Output current, A
I_{pv}	—	Photovoltaic current, A
I_{sc}	—	Short circuit current, A
$I_{pv,n}$	—	Light generated current, A
K	—	Boltzman constant, J/K
K_{Isc}	—	Temperature coefficient of short circuit current, %/°C
N_s	—	Number of cells connected in series
q	—	Charge of an electron, C
R_s	—	Series resistance factor, Ω
R_p	—	Shunt resistance factor, Ω
T	—	Actual cell temperature, °C, °K
T_{NOCT}	—	Nominal operating cell temperature, °C, °K
T_n	—	Nominal temperature, °C, °K
T_a	—	Ambient temperature, °C, °K
V	—	Output voltage, V
V_{oc}	—	Open circuit voltage, V
V_t	—	Thermal voltage, V

References

[1] S. Amaducci, X. Yin, M. Colauzzi, Agrivoltaic systems to optimise land use for electric energy production, Appl. Energy, 220 (2018) 545–561.
[2] A. Agotini, M. Colauzzi, S. Amaducci, Innovative agrivoltaic systems to produce sustainable energy: an economic and environmental assessment, Appl. Energy, 281 (2021) 116102, doi: 10.1016/j.apenergy.2020.116102.
[3] S. Touil, A. Richa, M. Fizir, B. Bingwa, Shading effect of photovoltaic panels on horticulture crops production: a mini review, Rev. Environ. Sci. Bio/Technol., 20 (2021) 281–296.
[4] H. Dinesh, J.M. Pearce, The potential of agrivoltaic systems, Renewable Sustainable Energy Rev., 54 (2016) 299–308.

[5] A.R.D.A. Zanella, E.D. Silva, L.C.P. Albini, Security challenges to smart agriculture: current state, key issues, and future directions, Array, 8 (2020) 100048, doi: 10.1016/j.array.2020.100048.
[6] S. Sumathi, S. Krishnan, Artificial intelligence for smart solar power irrigation: comprehensive review, Adv. Sci. Eng., 7 (2021) 1894–1903.
[7] M. Aliyu, G. Hassan, S.A. Said, M.U. Siddiqui, A.T. Alawami, I.M. Elamin, A review of solar-powered water pumping systems, Renewable Sustainable Energy Rev., 87 (2018) 61–76.
[8] S. Verma, S. Mishra, S. Chowdhury, A. Gaur, S. Mohapatra, A. Soni, P. Verma, Solar PV powered water pumping system – a review, Mater. Today: Proc., 33 (2020) 303–307.
[9] M. Gasque, P.G. Altozano, R.P.G. Colomer, Optimisation of the distribution of power from a photovoltaic generator between two pumps working in parallel, Sol. Energy, 198 (2020) 324–334.
[10] E.M. Salilih, Y.T. Birhame, S.H. Arshi, Performance analysis of DC type variable speed solar pumping system, Sol. Energy, 208 (2020) 1039–1047.
[11] B.A. Bhayo, H.H. Al-Kayiem, S.I. Gilani, Assessment of standalone solar PV-Battery system for electricity generation and utilization of excess power for water pumping, Sol. Energy, 194 (2019) 766–776.
[12] Renu, B. Bora, B. Prasad, O.S. Sastry, A. Kumar, M. Bangar, Optimum sizing and performance modeling of solar photovoltaic (SPV) water pumps for different climatic conditions, Sol. Energy, 155 (2017) 1326–1338.
[13] P. Santra, Performance evaluation of solar PV pumping system for providing irrigation through micro-irrigation techniques using surface water resources in hot arid region of India, Agric. Water Manage., 245 (2021) 106554, doi: 10.1016/j.agwat.2020.106554.
[14] S. Statkic, B. Jovanovic, A. Micic, N. Arsic, S. Jovic, Adaptive neuro fuzzy selection of the most important factors for photovoltaic pumping system performance prediction, J. Build. Eng., 30 (2020) 101242, doi: 10.1016/j.jobe.2020.101242.
[15] V. Sontake, A.K. Tiwari, V.R. Kalamkar, Performance investigations of solar photovoltaic water pumping system using centrifugal deep well pump, Therm. Sci., 24 (2019) 2915–2927.
[16] V.C. Sontake, A.K. Tiwari, V.R. Kalamkar, Experimental investigations on the seasonal performance variations of directly coupled solar photovoltaic water pumping system using centrifugal pump, Environ. Dev. Sustainability, 23 (2021) 8288–8306.
[17] M. Benghanem, K.O. Daffallah, A. Almohammedi, Estimation of daily flow rate of photovoltaic water pumping systems using solar radiation data, Results Phys., 8 (2018) 949–954.
[18] A.K. Tiwari, V.R. Kalamkar, Effects of of total head and solar radiation on the performance of solar water pumping system, Renewable Energy, 118 (2018) 919–927.
[19] S. Bana, R.P. Saini, Identification of unknown parameters of a single diode photovoltaic model using particle swarm optimization with binary contraint, Renewable Energy, 101 (2017) 1299–1310.
[20] E.M. Salilih, Y.T. Birhane, Modelling and performance analysis of directly coupled vapor compression solar refrigeration system, Sol. Energy, 190 (2019) 228–238.
[21] M. Premkumar, C. Kumar, R. Sowmya, Mathematical modelling of solar photovoltaic cell/panel/array based on the physical parameters from the manufacturer's datasheet, Renewable Energy Dev., 9 (2020) 7–22.
[22] M.G. Villalva, J.R. Gazoli, E.R. Filho, Comprehensive approach to modeling and simulation of photovoltaic arrays, IEEE Trans. Power Electron., 24 (2009) 1198–1208.
[23] M. Rasheed, O.Y. Mohammed, S. Shihab, A.A. Adili, A comparative analysis of PV cell mathematical model, J. Phys. Conf. Ser., 1795 (2021) 012042.
[24] M.T. Hagan, H.B. Demuth, M.H. Beale, O. Jesús, Neural Network Design, PWS Publishing Company, Boston, 1997.
[25] T.L. Fine, Feedforward Neural Network Methodology, Springer Science, New York, 1999.
[26] A. Sayed, M.E. Shimy, M.E. Metwally, M. Elshahed, Reliability, availability and maintainability analysis for grid-connected solar photovoltaic systems, Energies, 12 (2019) 1213, doi: 10.3390/en12071213.
[27] A. Altamimi, D. Jayaweera, Reliability of power systems with climate change impacts on hierarchical levels of PV systems, Electr. Power Syst. Res., 190 (2021) 106830, doi: 10.1016/j.epsr.2020.106830.
[28] H. Mahmoudi, O. Abdellah, N. Ghaffour, Capacity building strategies and policy for desalination using renewable energy in Algeria, Renewable Sustainable Energy Rev., 13 (2009) 921–926.

Appendix A – Experimental elecrical performance – PV Module JKM325M-60-V